

# Temperature-insensitive laser frequency locking near absorption lines

Cite as: Rev. Sci. Instrum. **82**, 033114 (2011); <https://doi.org/10.1063/1.3574221>

Submitted: 16 February 2011 . Accepted: 13 March 2011 . Published Online: 30 March 2011

Natalie Kostinski, Ben A. Olsen, Robert Marsland, Bart H. McGuyer, and William Happer



View Online



Export Citation

## ARTICLES YOU MAY BE INTERESTED IN

### [Small-sized dichroic atomic vapor laser lock](#)

Review of Scientific Instruments **82**, 043107 (2011); <https://doi.org/10.1063/1.3568824>

### [A microfabricated optically-pumped magnetic gradiometer](#)

Applied Physics Letters **110**, 031106 (2017); <https://doi.org/10.1063/1.4974349>

### [Chip-scale atomic devices](#)

Applied Physics Reviews **5**, 031302 (2018); <https://doi.org/10.1063/1.5026238>

**MCL**  
MAD CITY LABS INC.

AFM & NSOM      Nanopositioning Systems      Micropositioning      Single Molecule Microscopes

## Temperature-insensitive laser frequency locking near absorption lines

Natalie Kostinski,<sup>1,a)</sup> Ben A. Olsen,<sup>2</sup> Robert Marsland III,<sup>2</sup> Bart H. McGuyer,<sup>2</sup>  
and William Happer<sup>2</sup>

<sup>1</sup>*Department of Electrical Engineering, Princeton University, Princeton, New Jersey 08544, USA*

<sup>2</sup>*Department of Physics, Princeton University, Princeton, New Jersey 08544, USA*

(Received 16 February 2011; accepted 13 March 2011; published online 30 March 2011)

Combined magnetically induced circular dichroism and Faraday rotation of an atomic vapor are used to develop a variant of the dichroic atomic vapor laser lock that eliminates lock sensitivity to temperature fluctuations of the cell. Operating conditions that eliminate first-order sensitivity to temperature fluctuations can be determined by low-frequency temperature modulation. This temperature-insensitive gyrotropic laser lock can be accurately understood with a simple model, that is in excellent agreement with observations in potassium vapor at laser frequencies in a 2 GHz range about the 770.1 nm absorption line. The methods can be readily adapted for other absorption lines.

© 2011 American Institute of Physics. [doi:10.1063/1.3574221]

The dichroic atomic vapor laser lock (DAVLL),<sup>1–7</sup> based on the circular dichroism induced by a magnetic field in an atomic vapor, provides a continuous laser frequency locking range comparable to the width of the optical absorption line. Closely related locking methods use the Faraday rotation instead of the circular dichroism.<sup>8–10</sup> DAVLL systems work best if the locking frequency is that of vanishing circular dichroism, and locking systems based on Faraday rotation work best if the locking frequency is that of vanishing rotation. But one can lock to other frequencies in or near the atomic absorption line by shifting the orientation of the polarizing optics or by using differential amplification of the beam splitter channels. We will refer to locking systems that depend on circular dichroism or Faraday rotation, or some combination of the two effects<sup>11,12</sup> as gyrotropic laser locks (GLLs). Except for the “natural” locking frequencies of vanishing circular dichroism or vanishing Faraday rotation, the locking frequency is sensitive to temperature drifts. Here, we describe a GLL whose locking frequency is independent—in first order—to temperature fluctuations for any desired frequency close to the atomic absorption line.

A GLL system can be characterized by the complex phase shifts  $\phi_q = 2\pi k N \ell \alpha_q$  acquired by circularly polarized photons, propagating along the direction of the magnetic field, that change the azimuthal angular momentum of the atom by  $q = \pm 1$  on absorption. Here  $k = 2\pi/\lambda$  is the wavenumber for the light of wavelength  $\lambda$ ,  $\ell$  is the path length through the vapor,  $N$  is the number density of atoms, and  $\alpha_q$  is the atom polarizability for circularly polarized light. Below we refer to the mean phase,  $\bar{\phi} = (\phi_1 + \phi_{-1})/2$ , and the phase difference or “gyrotropic angle,”  $\Delta\phi = \Delta\phi' + i\Delta\phi'' = \phi_1 - \phi_{-1}$ . The gyrotropic angle of potassium vapor was calculated using computer codes adapted from Happer *et al.*<sup>13</sup> and plotted for the range of frequencies in Fig. 1.

GLL operation depends on the steep frequency dependence of  $\Delta\phi$ , but  $\Delta\phi$  also depends on temperature. Thus,

temperature fluctuations can be mistaken for frequency fluctuations by the feedback system. For saturated atomic vapors, all but a few percent of the  $\Delta\phi$  temperature dependence comes through  $N$ , and it is a good first approximation to write  $\partial\Delta\phi/\partial T = \Delta\phi \partial(\ln N)/\partial T$ . According to the Clausius-Clapeyron, equation,<sup>14</sup>  $\partial(\ln N)/\partial T = ([L/k_B T] - 1)/T$ , where  $L$  is the latent heat of vaporization per atom and  $k_B$  is Boltzmann’s constant. Because of the large latent heats (e.g.,  $L/k_B T \approx 30$  for potassium and rubidium) GLL systems require very precise temperature control if operated at frequencies other than the ideal locking frequencies of zero circular dichroism or zero Faraday rotation. For a typical, nonideal frequency for saturated potassium vapor at 60 °C, a temperature change of 1 °C changes  $\Delta\phi$  by 10% and shifts the lock frequency by  $\sim 100$  MHz. To hold the frequency stable to  $\pm 1$  MHz, the temperature must be held stable to  $\pm 0.01$  °C. Reeves *et al.*<sup>5</sup> recently observed that with properly chosen orientations of polarizing optics of a GLL and with differential attenuation of the two outputs of the beam splitter, one can eliminate the temperature sensitivity. Stimulated by this work we have completed a theoretical and experimental study of the GLL sketched in Fig. 2.

For our experiments, a linearly polarized beam of intensity  $I_0 = 55 \mu\text{W}/\pi(0.5 \text{ mm})^2$  is produced with an external-cavity diode laser in Littrow design (Toptica DL Pro 780, not shown) with a wavelength close to the 770.1 nm D1 ( $4^2\text{S}_{1/2} \rightarrow 4^2\text{P}_{1/2}$ ) transition of potassium. The beam traverses a zero-order half-wave ( $\lambda/2$ ) plate (Thorlabs WPH05M-780, not shown) that is used to vary the polarization angle  $\theta$  of the light with respect to an arbitrarily chosen  $x$  axis. This light then traverses a glass vapor cell with natural-abundance potassium metal and  $\sim 1$  Torr  $\text{N}_2$  buffer gas. The cell is housed within a solid brass oven and resistively heated to 60 °C by a seven-layer solenoid of copper wire which also provides a 150 G longitudinal magnetic field, similar to the apparatus described by McCarron *et al.*<sup>6</sup>

As it traverses the vapor, the light becomes elliptically polarized with tilt angle  $\beta$  and ellipticity parameter

<sup>a)</sup>Electronic mail: nkostins@princeton.edu.

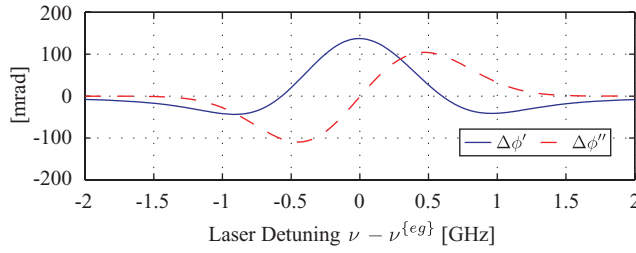


FIG. 1. (Color online) Real and imaginary parts of the gyrotropic angle  $\Delta\phi$  for a length  $\ell = 1.86$  cm of saturated potassium vapor (93.3%  $^{39}\text{K}$  and 6.7%  $^{41}\text{K}$ ) at temperature  $T = 60^\circ\text{C}$ , a magnetic field  $B = 150$  G, and a laser frequency  $\nu$  close to the zero-field mean frequency  $\nu^{(eg)}$  of the 770.1 nm line of  $^{39}\text{K}$ .

$\eta$ , given by the ratio of the semiminor to semimajor axes of the polarization ellipse. In terms of the gyrotropic angle,  $\beta = \theta - \Delta\phi'/2$  and  $\eta = \tanh(\Delta\phi''/2)$ . The light then passes through a zero-order quarter-wave ( $\lambda/4$ ) plate (Thorlabs WPQ05M-780) with slow axis at an angle  $\psi$  from the  $x$  axis before entering a Wollaston prism (Thorlabs WP-10) that separates the linear  $x$  and linear  $y$  polarization components into separate beams with relative intensities  $S_x = I_x/I_0$  and  $S_y = I_y/I_0$ . The beams are detected with a balanced photodetector (Thorlabs PDB210A) which produces a signal  $S \propto S_x - S_y$  as shown in Fig. 2.

For an operating cell temperature  $T_0$  and desired laser frequency  $\nu_0$ , the angles  $\theta$  and  $\psi$  can be chosen so that  $S_x = S_y$ , or equivalently,  $S = 0$ . For small deviations of the laser frequency near this point,  $S = (\nu - \nu_0) \partial S/\partial \nu$ . Provided  $\partial S/\partial \nu \neq 0$ ,  $S$  can be used as the error signal in a feedback loop to control the laser frequency so  $\nu = \nu_0$ .

Rewriting Eq. (2) of Yashchuk *et al.*<sup>11</sup> with our conventions for angles and phase retardations, we find

$$S = S_x - S_y = e^{-2\bar{\phi}''} K, \quad (1)$$

where

$$K = \cos 2\psi \cos(2\theta - 2\psi - \Delta\phi') + \sin 2\psi \sinh \Delta\phi''. \quad (2)$$

From inspection of Eq. (1) we see that for any locking frequency  $\nu_0$ , the locking criterion  $S = 0$  defines a functional relationship between the angles  $\theta$  and  $\psi$ . Any angle pair that satisfies  $S = 0$  and  $\partial S/\partial \nu \neq 0$  can be used to lock the laser to  $\nu_0$ , but different angle pairs have different sensitivities to temperature fluctuations. As pointed out by Reeves *et al.*,<sup>5</sup> the temperature sensitivity of the locking frequency  $\nu_0$  is given

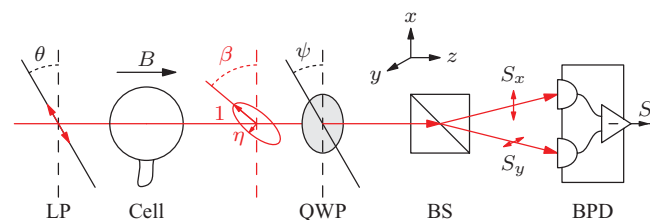


FIG. 2. (Color online) Experimental setup for the GLL. LP: Linearly polarized light,  $B$ : Applied magnetic field, QWP: Quarter-wave plate, BS: Beam splitter (Wollaston prism), BPD: Balanced photodetector.  $\theta$  is set by the input half-wave plate angle, and  $\psi$  is the QWP angle.

by

$$\frac{\partial \nu_0}{\partial T} = \frac{\partial S}{\partial T} \left( \frac{\partial S}{\partial \nu} \right)^{-1}. \quad (3)$$

Any angle pair for which  $\partial S/\partial T = 0$  will be a temperature insensitive point (TIP), as defined by Reeves *et al.* The GLL of Fig. 2 differs from that of Reeves *et al.* because of the additional requirement that the two channels of the beam splitter have equal intensities ( $S = 0$ ) at lock. From inspection of Eq. (1) we see that there are two angle pairs ( $\theta_{\pm}, \psi_{\pm}$ ) that simultaneously satisfy  $S = 0$  and  $\partial S/\partial T = 0$ ,

$$\psi_{\pm} = \pm \frac{\tan^{-1} y}{2}, \quad \theta_{\pm} = \psi_{\pm} + \frac{\Delta\phi' + \tan^{-1} z}{2}. \quad (4)$$

The argument  $y$  is given by

$$y = \frac{\left( \frac{\partial \Delta\phi'}{\partial T} \right)}{\sqrt{\left( \frac{\partial \Delta\phi'}{\partial T} \right)^2 \sinh^2 \Delta\phi'' + \left( \frac{\partial \Delta\phi''}{\partial T} \right)^2 \cosh^2 \Delta\phi''}} \quad (5)$$

and the argument  $z$  is given by

$$z = \frac{\left( \frac{\partial \Delta\phi''}{\partial T} \right) \cosh \Delta\phi''}{\left( \frac{\partial \Delta\phi'}{\partial T} \right) \sinh \Delta\phi''}. \quad (6)$$

To obtain smooth curves of  $\theta_{\pm}$  versus laser frequency, one must offset the expressions for  $\theta_{\pm}$  in Eq. (4) by “unwrapping angles”—multiples of  $90^\circ$  which change at the three frequencies where  $z = \pm\infty$ . The unwrapping angles account for the multiple values of the function  $\tan^{-1}$ .

To determine whether the operation of the GLL sketched in Fig. 2 is well described by the model outlined above, we carried out a series of experiments with the parameters mentioned in the caption of Fig. 1. To calibrate and monitor the laser frequency we used a second beam from the same laser which passed through a second potassium vapor cell with no buffer gas. By monitoring the absorption of the retro-reflected beam we generated Doppler-free saturated absorption signals which provided a precise frequency reference. The saturated-absorption signal was monitored on an oscilloscope during the experiments, while a second oscilloscope displayed the error signal  $S$ .

For several desired locking frequencies,  $\nu_0$ , we measured the angles  $\theta$  and  $\psi$  that produced  $S = 0$ . For each such pair, we modulated the laser frequency near  $\nu_0$  at 140 Hz and measured the modulation of  $S$  at that frequency with a lock-in amplifier to obtain a signal proportional to the feedback factor  $\partial S/\partial \nu$ . We also modulated the cell temperature by illuminating the cell through a small hole in the wall of the oven with 1 W of 532 nm laser light (from a Coherent Verdi V-10 laser), chopped on and off at 100 Hz. Multiple reflections from the oven walls helped to spread this light over most of the cell surface, in analogy with an integrating sphere. A filter before the balanced photodetector blocked any intensity reading from the 532 nm light. This simple procedure works because the droplets or films of alkali metal on the inner cell walls absorb visible light very efficiently as plasmon modes.<sup>15</sup> Any laser (for example, a high-power, green or blue laser pointer)

that can provide about 1 W of visible light should work as well as the one we used.

Neither the gas inside the cell nor the glass substrate can absorb appreciable amounts of visible light. The optical power heats the metal, which then heats the gas and a very thin layer of the substrate glass. The thermal diffusivities,  $D$  (in  $\text{cm}^2 \text{s}^{-1}$ ) of the gas (1 Torr  $\text{N}_2$ ), metal (potassium), and glass (pyrex) are  $D_g = 180$ ,  $D_m = 0.66$ , and  $D_p = 7.9 \times 10^{-3}$ , respectively. For heating of angular frequency  $\omega = 200\pi \text{ s}^{-1}$ , the attenuation lengths  $l = \sqrt{D/\omega}$  (in cm) for modulated heat waves induced in the three media are  $l_g = 0.54$ ,  $l_m = 0.0324$ , and  $l_p = 0.0035$ . The attenuation length for the gas being comparable to the cell radius, 1.25 cm, we expect the temperature modulation in the gas to be nearly spatially uniform. In contrast, the attenuation length of the glass is so small, 35  $\mu\text{m}$ , that the temperature modulation of the glass walls will be confined to a very thin layer near the inner surface. Thus, the majority of the heating occurs in the metal, and not in the glass walls or other parts of the oven, which have much higher heat capacities, and for which 100 Hz temperature modulation is impractically fast. The 100 Hz modulation of  $S$  that resulted from the temperature modulation of the potassium was detected using a second lock-in amplifier, yielding a signal proportional to  $\partial S/\partial T$ .

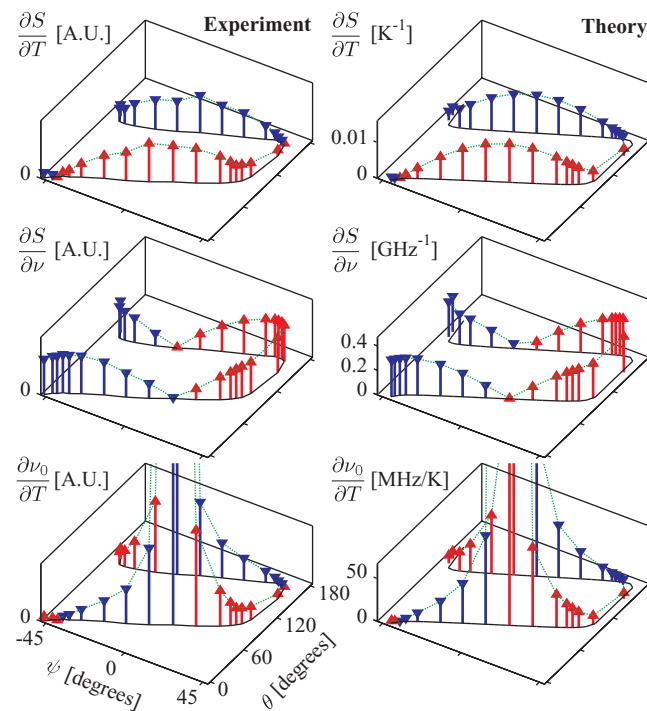


FIG. 3. (Color online) Comparison of experimental data for the locking device of Fig. 2 with model values following from Eq. (1). Positive values have red stems topped by upward triangles, and negative values have blue stems topped with downward triangles. The laser was detuned by  $\nu_0 - \nu^{(eg)} = 80 \text{ MHz}$ , and the other conditions were the same as for Fig. 1. TIP's in degrees, are  $(\theta_+, \psi_+) = (174, 39)$  and  $(\theta_-, \psi_-) = (6, -39)$ . The arbitrary units (A.U.) of the experimental data are lock-in amplifier voltages, scaled to be close to the model values on the right. The relative, experimental values of  $\partial S/\partial T$  and  $\partial S/\partial \nu$  are close to those of the model. When  $\partial S/\partial \nu = 0$ , the temperature sensitivity is infinite.

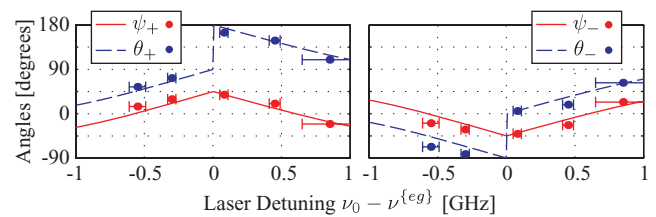


FIG. 4. (Color online) A comparison of measured (filled circles) and modeled (curves) temperature-insensitive points, obtained from experiments such as those of Fig. 3 for various locking frequencies  $\nu_0$ . The horizontal error bars represent uncertainty due to frequency calibration with saturated absorption signals.

The ratio of the two lock-in signals then gave  $\partial \nu_0/\partial T$  according to Eq. (3).

The results of these measurements are compared to theoretical values from Eqs. (1) and (2) in Fig. 3. Measurements such as those of Fig. 3 were repeated for a number of desired locking frequencies,  $\nu_0$ , and the measured angle pairs,  $(\theta_{\pm}, \psi_{\pm})$ , along with theoretical values from Eq. (4), are shown in Fig. 4. There is good agreement between experimentally measured and modeled values. Theory similar to that outlined above, shows that the temperature-insensitive GLL has a modest sensitivity to magnetic field,  $\partial \nu_0/\partial B \approx 1 \text{ MHz G}^{-1}$  ( $\nu_0 - \nu^{(eg)}$  GHz).

At their ideal locking frequencies, the DAVLL of Corwin *et al.*<sup>2</sup> and the balanced polarimeter of Yashchuk *et al.*<sup>11</sup> are limiting cases of the GLL described here. Setting  $\psi = 45^\circ$  in Eq. (2) we get the feedback signal,  $S = e^{-2\phi''} \sinh \Delta\phi''$ , of an ideal DAVLL.  $S$  vanishes for a frequency close to the center of the absorption line where  $\Delta\phi' = 0$  (zero circular dichroism), as one can see from Fig. 1. There is no temperature dependence,  $\partial \Delta\phi''/\partial T \approx \Delta\phi'' \partial(\ln N)/\partial T = 0$ , since  $\Delta\phi' = 0$ . With  $\psi = 0$  and  $\theta = 45^\circ$  we find the feedback signal,  $S = e^{-2\phi''} \sin \Delta\phi'$ , of an ideal balanced polarimeter.  $S$  vanishes for two frequencies, left and right of line center, where  $\Delta\phi' = 0$  (zero Faraday rotation). There is no temperature dependence,  $\partial \Delta\phi'/\partial T \approx \Delta\phi' \partial(\ln N)/\partial T = 0$ , since  $\Delta\phi' = 0$ . By introducing relative attenuation for the split beams of a DAVLL, or by changing the angle  $\theta$  away from  $45^\circ$  for a balanced polarimeter, these devices can operate for nonideal locking frequencies. The temperature sensitivities, proportional to  $\partial \Delta\phi''/\partial T \neq 0$  or  $\partial \Delta\phi'/\partial T \neq 0$ , are larger the more the desired locking frequency differs from the ideal frequency.

In conclusion, we have demonstrated that the GLL of Fig. 2 behaves as predicted by the simple formula Eq. (4), which gives the temperature-independent angles for any desired locking frequency. No optical attenuators, electrical offsets, or special temperature stabilization are needed. We also describe a convenient experimental method to fine-tune the temperature-independent angles.

<sup>1</sup>B. Chéron, H. Gilles, J. Hamel, O. Moreau, and H. Sorel, *J. Phys. III France* **4**, 401 (1994).

<sup>2</sup>K. L. Corwin, Z.-T. Lu, C. F. Hand, R. J. Epstein, and C. E. Wieman, *Appl. Opt.* **37**, 3295 (1998).

<sup>3</sup>N. Beverini, E. Maccioni, P. Marsili, A. Ruffini, and F. Sorrentino, *Appl. Phys. B* **73**, 133 (2001).

- <sup>4</sup>K. R. Overstreet, J. Franklin, and J. P. Shaffer, *Rev. Sci. Instrum.* **75**, 4749 (2004).
- <sup>5</sup>J. M. Reeves, O. Garcia, and C. A. Sackett, *Appl. Opt.* **45**, 372 (2006).
- <sup>6</sup>D. J. McCarron, I. G. Hughes, P. Tierney, and S. L. Cornish, *Rev. Sci. Instrum.* **78** (2007).
- <sup>7</sup>A. Millett-Sikking, I. G. Hughes, P. Tierney, and S. L. Cornish, *J. Phys. B* **40** (2007).
- <sup>8</sup>P. P. Sorokin, J. R. Lankard, V. L. Moruzzi, and A. Lurio, *Appl. Phys. Lett.* **15**, 179 (1969).
- <sup>9</sup>P. Siddons, N. C. Bell, Y. Cai, C. S. Adams, and I. G. Hughes, *Nature Photon.* **3**, 225 (2009).
- <sup>10</sup>A. L. Marchant, S. Händel, T. P. Wiles, S. A. Hopkins, C. S. Adams, and S. L. Cornish, *Opt. Lett.* **36**, 64 (2011).
- <sup>11</sup>V. V. Yashchuk, D. Budker, and J. R. Davis, *Rev. Sci. Instrum.* **71**, 341 (2000).
- <sup>12</sup>C. Lee, G. Z. Iwata, E. Corsini, J. M. Higbie, S. Knappe, M. P. Ledbetter, and D. Budker, arXiv:1012.3522v2.
- <sup>13</sup>W. Happer, Y.-Y. Jau, and T. Walker, *Optically Pumped Atoms* (Wiley-VCH, Weinheim, Germany 2010).
- <sup>14</sup>T. J. Killian, *Phys. Rev.* **27**, 578 (1926).
- <sup>15</sup>M. Blaber, M. Arnold, N. Harris, M. Ford, and M. Cortie, *Physica B* **394**, 184 (2007).